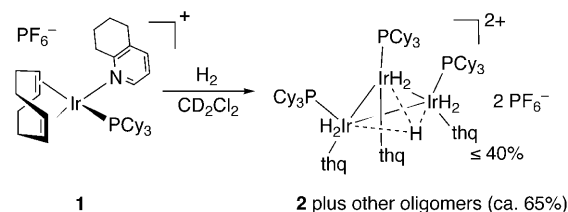


# Tetrameric Iridium Hydride-Rich Clusters Formed under Hydrogenation Conditions\*\*

Yingjian Xu, Mehmet A. Celik, Amber L. Thompson, Hairong Cai, Mine Yurtsever, Barbara Odell, Jennifer C. Green, D. Michael P. Mingos, and John M. Brown\*

Asymmetric hydrogenation using iridium catalysts has been recognized as an important alternative to rhodium catalysis in recent years, because it enables the creation of a new stereogenic center without reliance on polar functionality in the substrate.<sup>[1]</sup> Previous study of Ir hydrogenations provided significant insights into the mechanism,<sup>[2]</sup> and underscored that an important deactivation process involves the formation of catalytically inactive trimers.<sup>[3]</sup> The formation of such species may be limited by a judicious choice of nitrogen and phosphorus ligands, which leads to a new family of active catalysts. Herein, we highlight a quite different aspect of these studies. Hydrogenation of a specific iridium procatalyst under substrate free conditions leads not only to trimers but also higher nuclearity hydride-rich cluster compounds of iridium. Weller and McIndoe demonstrated that hydride-rich cluster compounds of rhodium have interesting structural and chemical features, but the corresponding compounds of iridium have not previously been studied.<sup>[4]</sup> Herein, we describe the unique structures of two tetrameric hydride-rich iridium clusters which are formed irreversibly under substrate-free conditions, in addition to a conventional trimer, as previously described (Scheme 1). The research suggests an important general route to this class of cluster compounds, because the nuclearities of the clusters formed under these conditions may in future be fine-tuned by varying the steric and electronic properties of the ligands.

Hydrogenation of complex **1** ( $[\text{Ir}(\text{PCy}_3)(\text{cod})-(\text{C}_9\text{H}_{11}\text{N})]\text{PF}_6$ ) in  $\text{CD}_2\text{Cl}_2$  was monitored by  $^1\text{H}$  NMR spectroscopy, until the reduction of 1,5-cyclooctadiene (cod) was



**Scheme 1.** Hydrogenation of complex **1** under ambient substrate-free conditions.

complete. At this stage, the  $^1\text{H}$  NMR spectrum showed a complex iridium hydride region, in which the species **2** (an analogue of the dicationic Crabtree trimer<sup>[3a]</sup>) was detected, although it provided  $\leq 40\%$  of the total signal intensity. The high resolution electrospray (ES) mass spectrum of solutions analyzed after complete reduction also revealed the presence of the standard trimer  $[\text{Ir}_3\text{H}_7(\text{PCy}_3)_3(\text{C}_9\text{H}_{11}\text{N})_3]^{2+}$  (**2**), and an ion formed by loss of one N ligand from **2**. In addition, two strong peaks corresponding to  $[\text{Ir}_4\text{H}_{10}(\text{PCy}_3)_4(\text{C}_9\text{H}_{11}\text{N})_2]^{2+}$  (**3a**) and  $[\text{Ir}_4\text{H}_{11}(\text{PCy}_3)_4(\text{C}_9\text{H}_{11}\text{N})]^+$  (**3b**) were observed. Both of these gave characteristic patterns based on the stable isotope ratio ( $^{191}\text{Ir}/^{193}\text{Ir} = 37.3:62.7$ ), providing unambiguous confirmation of the cation formulae (Figure 1).

The structure obtained by single-crystal X-ray diffraction, after very slow crystallization of the hydrogenation product from dichloromethane/pentane, corresponds to the complex **3a**,  $[\text{Ir}_4\text{H}_{10}(\text{C}_9\text{H}_{11}\text{N})_2]^{2+}(\text{PF}_6^-)_2$ .<sup>[5]</sup> The hydrogen atoms could not be located in the difference map, owing to the close proximity of heavy atoms and the associated termination

[\*] Dr. Y. Xu, Dr. A. L. Thompson, H. Cai, Dr. B. Odell, Prof. D. M. P. Mingos, Dr. J. M. Brown  
Chemistry Research Laboratory, Oxford University  
12 Mansfield Rd., Oxford OX1 3TA (UK)  
Fax: (+44) 1865-285-002  
E-mail: john.brown@chem.ox.ac.uk  
Homepage: <http://www.chem.ox.ac.uk/researchguide/jbrown.html>  
Prof. J. C. Green  
Inorganic Chemistry Laboratory, Oxford University (UK)

M. A. Celik, Prof. M. Yurtsever  
Istanbul Technical University, Faculty of Arts & Science (Turkey)

[\*\*] We thank Merck for an unrestricted grant (Y.X.) and Oxford and Istanbul Technical Universities (ITU-HPCC) for computing facilities. TÜBİTAK provided a six-month scholarship that enabled M.A.C. to work in Oxford in 2007. We gratefully acknowledge help from Dr. T. D. W. Claridge (NMR); Dr. N. Oldham and Dr. J. McCullagh (MS). Johnson-Matthey kindly provided a loan of iridium salts. Prof. Andrew Weller provided very helpful comments on this manuscript.

Supporting Information for this article is available on the WWW under <http://dx.doi.org/10.1002/anie.200804484>.

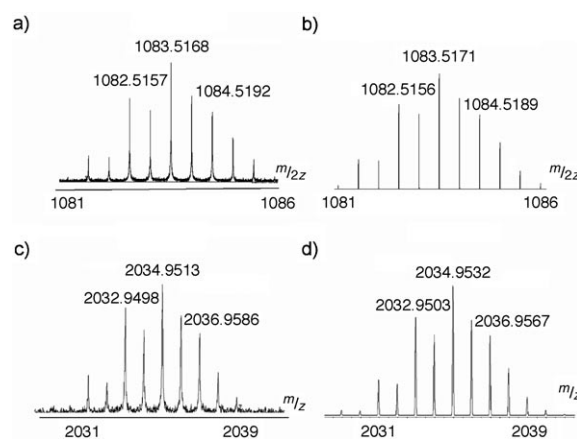


**Figure 1.** a) Experimental and b) calculated ES mass spectra for the  $[\text{Ir}_4\text{H}_{10}(\text{PCy}_3)_4(\text{C}_9\text{H}_{11}\text{N})_2]^{2+}$  dication **3a**. c) Experimental and d) calculated ES mass spectra for the  $[\text{Ir}_4\text{H}_{11}(\text{Cy}_3\text{P})_4(\text{C}_9\text{H}_{11}\text{N})]^+$  cation **3b**.

errors, but the non-hydrogen atom positions are clearly defined. The central iridium core of the cation consists of a butterfly motif with a  $C_2$  axis perpendicular to the Ir2–Ir2' hinge. Each Ir center is coordinated by  $PCy_3$  (Cy = cyclohexyl) ligands, with tetrahydroquinoline (THQ) ligands bound to the two terminal Ir centers. The location of the hydrogen atoms was computed by density functional (DFT) calculations, using  $PMe_3$  and pyridine as model ligands. Starting from the coordinates of the heavy atom core, which were allowed to relax, trial structures with differing hydrogen positions were optimized.<sup>[6a]</sup> Three low-energy structures within  $1 \text{ kJ mol}^{-1}$  of one another were located; they had similar core structures, with different rotameric forms of  $PMe_3$ . The structure that resembled the X-ray conformation most closely (Figure 2b) retained symmetry, with the  $C_2$  axis passing

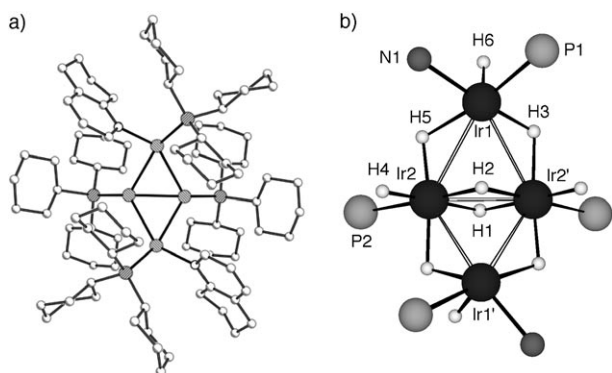


**Figure 2.** a) Molecular structure of complex **3a** as its  $CH_2Cl_2$  solvate,  $[C_{30}H_{164}N_2P_4Ir_4](PF_6)_2 \cdot 2CH_2Cl_2$  determined by single-crystal X-ray diffraction. Counterions, solvent molecules, carbon atoms, and hydrogen atoms are omitted for clarity (see the Supporting Information for full details). b) The core structure arising from DFT calculations on  $[Ir_4H_{10}(Me_3P)_4(C_5H_5N)_2]^{2+}$ .

through the two hydrogen atoms, which bridged the hinge iridium atoms Ir2 and Ir2'. It also confirmed the key experimental features (see Table 1), although Ir–Ir bond lengths were  $0.06\text{--}0.1 \text{ \AA}$  greater than the values given by X-ray diffraction (Table 1). The octahedral and square-pyramidal environments about the iridium centers indicated localized  $18e$  (Ir2, Ir2') and  $16e$  (Ir1, Ir1') iridium(III) centers. For comparison, the DFT-optimized structure of the model trimer  $[Ir_3H_7(PMe_3)_3py_3]^{2+}$  is included in the Supporting Information. Aside from the triple bridge, the hydrogen positions were not revealed by X-ray diffraction.

**Table 1:** Comparison of bond lengths and angles afforded by single-crystal X-ray diffraction (XRD) and density functional calculations (DFT) for **3a**.

Distance [Å]	XRD	DFT	Angle [°]	XRD	DFT
Ir1–Ir2	2.7703(6)	2.879	N1–Ir1–P1	94.7(3)	93.9
Ir2–Ir2'	2.6241(4)	2.686	N1–Ir1–Ir2	92.1(3)	98.0
Ir1–P1	2.284(3)	2.299	P1–Ir1–Ir2	109.4(1)	104.0
Ir1–N1	2.099(6)	2.119	P2–Ir2–Ir2'	140.3(1)	137.2
Ir2–P2	2.275(3)	2.299	Ir2–Ir1–Ir2'	56.17(2)	55.9

The  $^1H$ NMR spectrum of the hydrogenation product revealed signals in the Ir–H region corresponding to **3a**, albeit as the minor component (Figure 3, italicized *H*). The

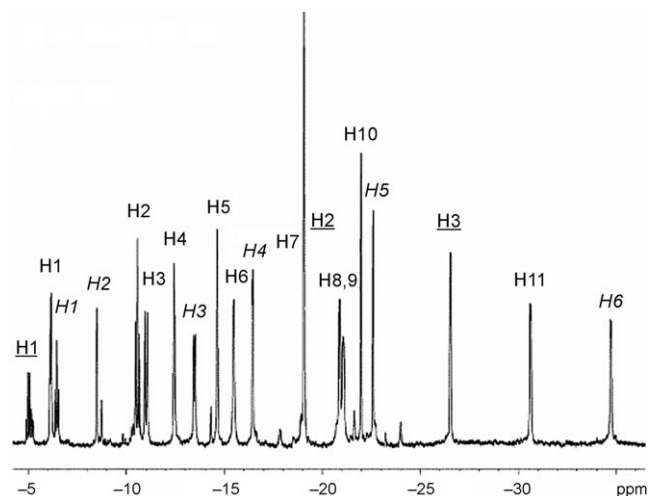


**Figure 3.**  $^1H$ NMR spectrum at 283 K of a typical reaction mixture, derived from hydrogenation of complex **2** in  $CD_2Cl_2$  in the region  $\delta = -5$  to  $-35$  ppm. The trimer signals are shown as underlined *H*, the dication **3a** as italic *H*, and the monocation **3b** as plain *H*.

two central bridging hydrides *H1* and *H2* are apparent at  $\delta = -6.46$  and  $-8.48$  ppm, and the other two pairs of bridging hydrides *H3* and *H5* at  $\delta = -13.46$  and  $-22.59$  ppm. The terminal hydrides *H4* and *H6* resonate at  $\delta = -16.44$  and  $-34.74$  ppm respectively. The signals all correlate with the expected phosphorus resonances [P1:  $\delta = 18.0$  ppm; P2:  $\delta = 60.5$  ppm]. These results provide support for the proposed structure.

The same spectrum demonstrated that the major species was a monocation with eleven inequivalent hydrides (Figure 3, plain *H*). A combination of X-ray crystallographic analysis, detailed NMR spectroscopic studies, and DFT calculations proved necessary before this structure could be fully defined. The ambient temperature  $^1H$ NMR spectrum shows four of the hydride resonances are broad and exchanging, namely *H1*, *H3*, *H4*, and *H6*. Only *H2* and *H6* make NOE contacts with aromatic protons of the thq ligand. *H2* resembles *H1* of the dication **3a**, and *H11* likewise resembles *H6* of the dication. With the exception of *H4* (see below), all of the protons can be assigned to an iridium partner by  $\{^{31}P\text{--}^1H\}$  correlation spectroscopy and, in the case of *H2*, *H5*, *H7*, and *H10*, further bridging was evident. When a hydrogenated sample was diluted with MeOH, a yellow precipitate was formed, affording a cleaner  $^1H$ NMR spectrum on redissolution in  $CD_2Cl_2$ . X-ray diffraction of the sample, recrystallized from  $CD_2Cl_2$ /pentane, gave a new structure, confirmed to be the monocationic complex **3b**,  $[Ir_4H_{11}(Cy_3P)_4(C_9H_{11}N)]^+PF_6^-$ .<sup>[5]</sup> Again, structural refinement located heavy atoms and the counterion, but not the hydrogen atoms. In the derived structure, the four iridium atoms are close to coplanarity (Figure 4a). This new structure indicates the formal replacement of one thq ligand (in the structure of

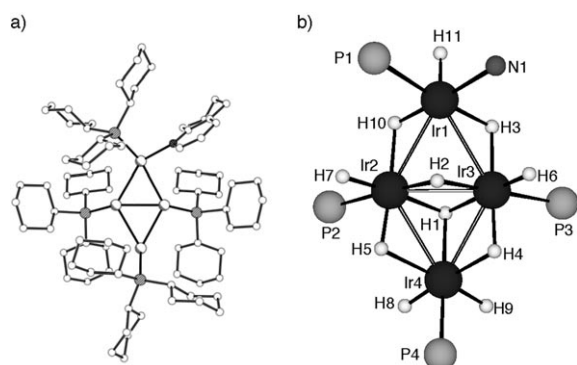


**Figure 4.** a) Molecular structure of complex **3b**  $[\text{C}_{81}\text{H}_{154}\text{NP}_4\text{Ir}_4]\text{PF}_6$  determined by single-crystal X-ray diffraction. Counterions, carbon atoms, and hydrogen atoms are omitted for clarity (see the Supporting Information for full details). b) Core structure from DFT calculations on  $[\text{Ir}_4\text{H}_{11}(\text{Me}_3\text{P})_4(\text{C}_5\text{H}_5\text{N})]^+$ .

**3a**) by a hydride ion. Initial attempts to simulate the experimental structure by DFT failed. Having established the X-ray crystal structure, modeling was attempted based on acceptable Ir–H and C–H contact distances, utilizing the full range of NMR spectroscopic data. DFT calculations based on this structure converged to an acceptable minimum (Figure 4b, Table 2).<sup>[6a]</sup> The model predicts that H4, one of the exchanging set, is bound to Ir4. In the heteronuclear correlation spectrum, H4 exhibits weak coupling to P1. This apparent contradiction is resolved by calculations that predict the detected long-range coupling between H4 and P1.<sup>[6b]</sup> The structure is based on localized octahedral geometries at Ir2, Ir3, and Ir4, and a square pyramidal geometry at Ir1, that is, a capping of the H2–Ir2–H1–Ir3 moiety so that H1 forms a third bridge to Ir4.

In this model, the four exchanging hydrogen atoms (identified by exchange spectroscopy, EXSY) are arranged in a square around Ir3. Detailed analysis of the exchange process,<sup>[7]</sup> exciting each of the four hydrogen atoms in turn, revealed a defined exchange pathway. Each proton undergoes primary exchange with its two neighbors, and only indirectly with the *trans* proton. The data for the four EXSY experiments (Figure 5) show a set of points representing exchange with the two *cis* protons (a), and a second set representing the secondary exchange process with the *trans* proton (b), and demonstrates the operation of a single mechanism involving

**Table 2:** Comparison of bond lengths and angles afforded by single-crystal X-ray diffraction (XRD) and density functional calculations (DFT) for **3b**.

Distance [Å]	XRD	DFT	Angle [°]	XRD	DFT
Ir1–Ir2	2.7785(4)	2.823	N1–Ir1–P1	93.9(2)	92.8
Ir1–Ir3	2.7421(4)	2.817	P1–Ir1–Ir2	106.33(6)	99.8
Ir2–Ir3	2.6758(4)	2.744	P1–Ir1–Ir3	152.87(6)	148.0
Ir2–Ir4	2.7748(4)	2.821	Ir2–Ir4–Ir3	58.18(1)	58.5
Ir3–Ir4	2.7281(4)	2.798	Ir2–Ir1–Ir3	57.98(1)	58.2
Ir1–P1	2.300(2)	2.314	Ir4–Ir3–Ir1	122.77(1)	121.1
Ir2–P2	2.269(2)	2.298	Ir1–Ir2–Ir4	119.70(1)	121.0
Ir3–P3	2.285(2)	2.291	P3–Ir3–Ir2	144.90(6)	143.0
Ir4–P4	2.200(2)	2.249	P2–Ir2–Ir3	140.62(5)	140.7
Ir1–N1	2.129(8)	2.130	P4–Ir4–Ir2	132.03(6)	133.5

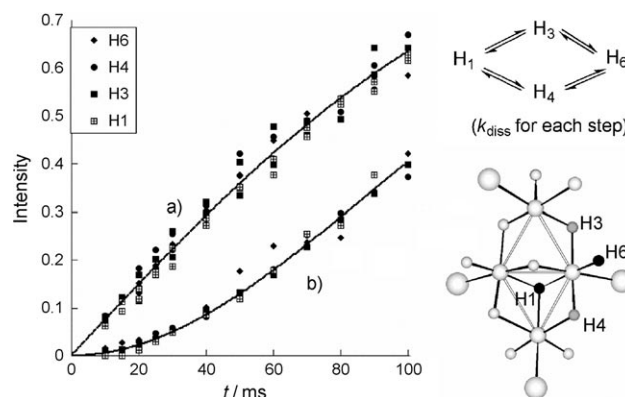


**Figure 5.** Results of the four EXSY exchange experiments at 288 K in  $\text{CD}_2\text{Cl}_2$  (see text for details). Each nucleus, H<sub>1</sub>, H<sub>3</sub>, H<sub>4</sub>, and H<sub>6</sub>, is irradiated in turn, and the three remaining in the exchanging set detected over the mixing time range  $t = 10$ –500 ms (shown here to  $t = 100$  ms). The superimposed lines represent simulation of the process illustrated, with  $k_{\text{diss}} = 7.5 \text{ s}^{-1}$ .  $\tau_1$  (the proton spin-lattice relaxation time) for the four exchanging hydrides was  $(310 \pm 25)$  ms. The molecular structure (right) shows *trans* pairs of exchanging protons in black and gray.

rotation about the P3–Ir3–H2 axis. Each dissociation step ( $k_{\text{diss}} = 7.5 \text{ s}^{-1}$ ) permits only one rotation, but equally in both directions.

The two tetramers **3a** and **3b** have distinct geometries, which may be understood by considering the bridging hydrides that form the structural links between pairs of iridium nuclei. The elevation view of dication **3a**, along the axis of the butterfly hinge (Figure 6), shows that the two terminal Ir and four bridging hydrides exhibit a boat conformation. For the monocation **3b**, the same view demonstrates a chair conformation, explaining why the Ir atoms in this complex are close to coplanar (XRD hinge angles  $40.8(1)^\circ$  for **3a** and  $9.4(1)^\circ$  for **3b**). Both **3a** and **3b** have 56 valence electrons, consistent with the cluster electron-counting rules for Pt-metal clusters with hydrido ligands. Planar and hinged butterfly structures are not distinguished by these rules.<sup>[8]</sup>

The distinction between precursor complex **1** and the original Crabtree catalyst **4**,<sup>[3a]</sup>  $[(\text{Cy}_3\text{P})(\text{C}_5\text{H}_5\text{N})\text{Ir}(\text{cod})]^+\text{PF}_6^-$  is simply the replacement of pyridine by tetrahydroquinoline, and the differences are likely to arise from steric rather than electronic factors. We considered the possibility that tetramers could also have been formed in the original work that led to trimer characterization. On repeating the hydrogenation procedure using complex **4**, the ES mass spectrum of the resulting solution clearly shows the presence of such a species. Only the N-dissociated tetrameric dication based on a  $\{\text{NP}_4\text{Ir}_4\}^{2+}$  core is detected, identified by its distinctive half-

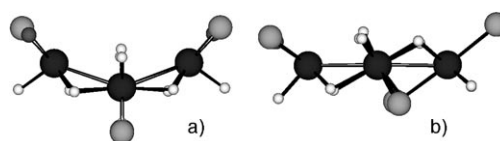


**Figure 6.** Elevation views of the two tetrameric complexes: a) **3a** and b) **3b**, emphasizing the origins of their geometric differences.

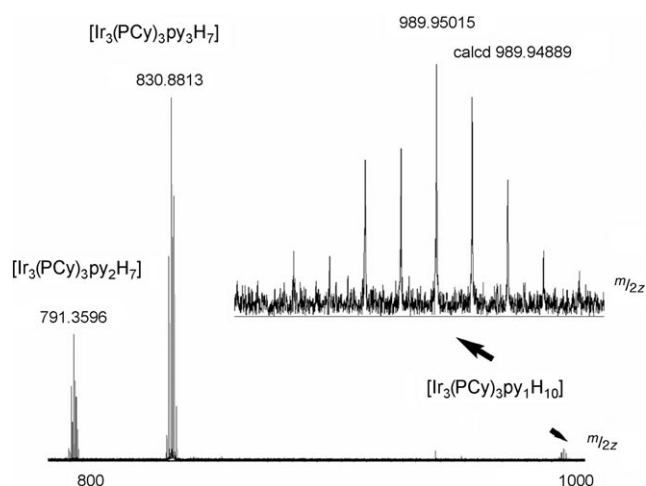


**Figure 7.** ES mass spectrum of hydrogenated Crabtree's catalyst,  $[(\text{cod})\text{Ir}(\text{PCy}_3)(\text{C}_5\text{H}_5\text{N})]\text{PF}_6$  (**4**, cod = 1,5-cyclooctadiene), showing the presence of tetrameric dication  $[\text{Ir}_4\text{H}_{10}(\text{Cy}_3\text{P})_4(\text{C}_5\text{H}_5\text{N})]^{2+}$ .

integer isotope pattern at 4% of the intensity of the main trimer peak (Figure 7).

Complexes **3a** and **3b** represent novel additions both to iridium chemistry,<sup>[9]</sup> and the emerging field of high hydride-content clusters. Structures with similar core geometries are uncommon.<sup>[10]</sup> Ligand-free iridium tetramers are known in the gas-phase, and the most stable form of naked  $\text{Ir}_4$  is square.<sup>[11]</sup> The closest condensed phase analogies, both in the nature of the preparative routes and the high hydrogen content of the products, arise extensive work by Weller and co-workers on cationic  $\text{Rh}_{6-8}$  phosphine hydride clusters.<sup>[12,13]</sup> Adams and co-workers have demonstrated the hydrogen uptake capabilities of mixed PtRh and PtOs clusters.<sup>[14]</sup> The sensitivity of our hydrogenation product structure to the nature of the nitrogen ligand in this work suggests that a rich iridium hydride cluster chemistry is accessible.

Received: September 11, 2008

Published online: December 9, 2008

**Keywords:** cluster compounds · hydrogenation · iridium · mass spectrometry · N ligands

- [1] Reviews: a) S. J. Roseblade, A. Pfaltz, *Acc. Chem. Res.* **2007**, *40*, 1402–1411; b) S. J. Roseblade, A. Pfaltz, *C. R. Chim.* **2007**, *10*, 178–187; c) T. L. Church, P. G. Andersson, *Coord. Chem. Rev.* **2008**, *252*, 513–531.
- [2] Y. Xu, D. M. P. Mingos, J. M. Brown, *Chem. Commun.* **2008**, 199–201.
- [3] a) D. F. Chodosh, R. H. Crabtree, H. Felkin, S. Morehouse, G. E. Morris, *Inorg. Chem.* **1982**, *21*, 1307–1311; b) H. H. Wang, L. H. Pignolet, *Inorg. Chem.* **1980**, *19*, 1470–1480; c) A. L. Casalnuovo, L. H. Pignolet, J. W. A. van der Velden, J. J. Bour, J. J. Steggerda, *J. Am. Chem. Soc.* **1983**, *105*, 5957–5958; d) H. H. Wang, A. L. Casalnuovo, B. J. Johnson, A. M. Mueting, L. H. Pignolet, *Inorg. Chem.* **1988**, *27*, 325–331; e) S. P. Smidt, A. Pfaltz, E. Martinez-Viviente, P. S. Pregosin, A. Albinati, *Organometallics* **2003**, *22*, 1000–1009.

- [4] a) A. S. Weller, J. S. McIndoe, *Eur. J. Inorg. Chem.* **2007**, 4411–4423; b) P. J. Dyson, J. S. McIndoe, *Angew. Chem.* **2004**, *116*, 6152–6154; *Angew. Chem. Int. Ed.* **2004**, *43*, 6028–6030.
- [5] CCDC 692069 and 692070 contain the supplementary crystallographic data for this paper. These data can be obtained free of charge from The Cambridge Crystallographic Data Centre via [www.ccdc.cam.ac.uk/data\\_request/cif](http://www.ccdc.cam.ac.uk/data_request/cif). Crystallographic data: **3a**:  $\text{C}_{90.75}\text{H}_{165.50}\text{Cl}_{1.50}\text{F}_{12}\text{Ir}_4\text{N}_2\text{P}_6$ ;  $M_r = 2493.48$ ; crystal size  $0.04 \times 0.11 \times 0.13$  mm; monoclinic ( $C_2$ );  $a = 22.8325(3)$ ,  $b = 17.2007(3)$ ,  $c = 16.6365(3)$  Å;  $\beta = 118.473(1)^\circ$ ;  $V = 5743.42(16)$  Å<sup>3</sup>;  $Z = 2$ ;  $\mu = 4.794$  mm<sup>-1</sup>;  $\rho_{\text{calcd}} = 1.457$  g cm<sup>-3</sup>;  $T = 150(2)$  K; 45 368 reflections measured; 1296 independent reflections ( $R_{\text{int}} = 0.1119$ );  $R1 = 0.0708$ ;  $wR2 = 0.1730$  [ $I > 2\sigma(I)$ ];  $\Delta\rho_{\text{min}} = -2.841$ ,  $\Delta\rho_{\text{max}} = 5.995$  e Å<sup>-3</sup>. **3b**:  $\text{C}_{82}\text{H}_{160.5}\text{Cl}_2\text{F}_6\text{Ir}_4\text{N}_1\text{O}_{3.25}\text{P}_5$ ;  $M_r = 2316.83$ ; crystal size  $0.08 \times 0.12 \times 0.14$  mm; triclinic ( $P\bar{1}$ );  $a = 14.59410(10)$ ,  $b = 17.6600(2)$ ,  $c = 20.9926(2)$  Å;  $\alpha = 108.3094(5)$ ,  $\beta = 103.8296(4)$ ,  $\gamma = 93.7822(5)^\circ$ ;  $V = 4928.91(8)$  Å<sup>3</sup>;  $Z = 2$ ;  $\mu = 5.570$  mm<sup>-1</sup>;  $\rho_{\text{calcd}} = 1.553$  g cm<sup>-3</sup>;  $T = 150(2)$  K; 37 501 reflections measured; 22 323 independent reflections ( $R_{\text{int}} = 0.115$ );  $R1 = 0.0557$ ;  $wR2 = 0.1450$  [ $I > 2\sigma(I)$ ];  $\Delta\rho_{\text{min}} = -3.69$ ,  $\Delta\rho_{\text{max}} = 4.09$  e Å<sup>-3</sup>.
- [6] a) Geometry optimizations of the Ir tetramers were carried out by density functional theory (DFT) methods with the empirically parameterized hybrid functional B3LYP as implemented in Gaussian 03. The equilibrium structures have been characterized by a lack of imaginary vibrations. The 6-31g(d) basis set was applied to all elements except Ir which is described with the LANL2DZ basis set; b) NMR spectroscopic calculations were carried out using the ADF 2007.01 program suite: ADF2007.01, SCM, Theoretical Chemistry, Vrije Universiteit, Amsterdam, The Netherlands, <http://www.scm.com>. Further details are given in the Supporting Information.
- [7] H. Hu, K. Krishnamurthy, *J. Magn. Reson.* **2006**, *182*, 173–177; MacKinetics (Leipold Associates) was used for the data simulation in Figure 5.
- [8] D. M. P. Mingos, A. S. May in *The Chemistry of Metal Cluster Complexes* (Ed.: D. F. Shriver, H. D. Kaesz, R. D. Adams), VCH, Weinheim, **1990**, pp. 11–119.
- [9] For a tetrahedral tetrameric hydride,  $[\text{Ir}_4\text{H}_8(\text{CO})_4(\text{PPh}_3)_4]$ , see: L. Garlaschelli, F. Greco, G. Peli, M. Manassero, M. Sansoni, R. Gobetto, L. Salassa, R. D. Pergola, *Eur. J. Inorg. Chem.* **2003**, 2108–2112.
- [10] a) For a butterfly  $\text{Pt}_4$  cationic heptahydride tetramer see: R. J. Goodfellow, E. M. Hamon, J. A. K. Howard, J. L. Spencer, D. G. Turner, *J. Chem. Soc. Chem. Commun.* **1984**, 1604–1606; b) for a planar rhomboidal  $\text{Re}_2\text{Au}_2$  tetrameric hexahydride see: B. R. Sutherland, D. M. Ho, J. C. Huffman, K. G. Caulton, *Angew. Chem.* **1987**, *99*, 147–149; *Angew. Chem. Int. Ed. Engl.* **1987**, *26*, 135–137.
- [11] V. Stevanovic, Z. Sljivancanin, A. Baldereschi, *Phys. Rev. Lett.* **2007**, *99*, 165501–165504.
- [12] a) M. J. Ingleson, M. F. Mahon, P. R. Raithby, A. S. Weller, *J. Am. Chem. Soc.* **2004**, *126*, 4784–4785; b) S. K. Brayshaw, M. J. Ingleson, J. C. Green, J. S. McIndoe, P. R. Raithby, G. Kociok-Koehn, A. S. Weller, *J. Am. Chem. Soc.* **2006**, *128*, 6247–6263; c) S. K. Brayshaw, J. C. Green, R. Edge, E. J. L. McInnes, P. R. Raithby, J. E. Warren, A. S. Weller, *Angew. Chem.* **2007**, *119*, 7990–7994; *Angew. Chem. Int. Ed.* **2007**, *46*, 7844–7848, and intervening references.
- [13] A combination of NMR spectroscopy and DFT calculations was also used to define the hydride positions of unsymmetrical cationic  $[\text{Rh}_6\text{P}_6\text{H}_n]$  ( $n = 12, 14, 16$ ) clusters: S. K. Brayshaw, J. C. Green, N. Hazari, A. S. Weller, *Dalton Trans.* **2007**, 1781–1792.
- [14] R. D. Adams, B. Captain, M. D. Smith, *Angew. Chem.* **2006**, *118*, 1127–1130; *Angew. Chem. Int. Ed.* **2006**, *45*, 1109–1112; R. D. Adams, B. Captain, L. Zhu, *J. Am. Chem. Soc.* **2007**, *129*, 2454–2455.